Advance in Biological Research, 2025, 6(1), 1-13
https://www.hillpublisher.com/journals/abr/
ISSN Online: 2635-0319

Construction and Validation of a Prognostic Model for Immune and Metabolism-related Genes in Laryngeal Squamous Cell Carcinoma

Zhenlian Xie[1], Shiwei Gong[3], Zhang Feng[2,*]

[1]Department of Oncology, Pingnan County People's Hospital, Guigang 537300, Guangxi, China.
[2]Department of Otolaryngology Head and Neck Surgery, Pingnan County People's Hospital, Guigang 537300, Guangxi, China.
[3]Department of Oncology, Guilin Hospital, Xiangya Second Hospital, Central South University, Guilin 541001, Guangxi, China.

How to cite this paper: Zhenlian Xie, Shiwei Gong, Zhang Feng. (2025). Construction and Validation of a Prognostic Model for Immune and Metabolism-related Genes in Laryngeal Squamous Cell Carcinoma. *Advance in Biological Research*, 6(1), 1-13.
DOI: 10.26855/abr.2025.06.001

Received: July 15, 2025
Accepted: August 8, 2025
Published: September 5, 2025

Corresponding author: Zhang Feng, Department of Otolaryngology Head and Neck Surgery, Pingnan County People's Hospital, Guigang 537300, Guangxi, China.

Abstract

Background: Laryngeal squamous cell carcinoma (LSCC) is an aggressive malignant tumor, characterized by high incidence and mortality. Metabolic reprogramming is an emerging hallmark of cancer that affects the tumor microenvironment (TME) by modulating the biological behavior of cancer and immune cells. Metabolism and immunity may jointly participate in the progression of LSCC to some extent. The purpose of this study is to explore the predictive value of immune and metabolic-related genes in laryngeal cancer and their complex interactions with the TME. **Methods:** Gene expression data, mutation data, and clinical information of LSCC were acquired from The Cancer Genome Atlas (TCGA) and Gene Expression Omnibus (GEO). Subsequently, differentially expressed genes (DEGs) related to immunity and metabolism were identified, and functional enrichment analysis was conducted to explore their underlying mechanisms. We utilized Cox and LASSO regression analyses to develop a risk signature for immune and metabolism-related genes (IMRGs), which was then validated in TCGA and GEO cohorts. The association of the risk score with clinical characteristics, somatic mutations, microenvironmental features, and drug sensitivity was further investigated through correlation analyses. **Results:** A prognostic model composed of three genes (ARG2, PLCG1, TKFC) was constructed, with the high-risk score subgroup exhibiting poorer prognosis. The analysis of the ROC curve indicated that the prognostic model possesses strong predictive power (AUC = 0.655). Additionally, the risk score is an independent prognostic factor, and it is closely related to somatic mutations, immune microenvironment, and drug sensitivity. **Conclusions:** A prognostic model associated with immune and metabolism was established for LSCC based on three key genes. This model is proficient in accurately predicting outcomes for individuals suffering from LSCC. Furthermore, this prognostic model has demonstrated significant potential in uncovering immunological characteristics, evaluating the efficacy of immunotherapies, identifying somatic mutations, and predicting drug sensitivities.

Keywords

Laryngeal squamous cell carcinoma; immune; metabolism; prognosis; immune microenvironment; drug prediction

1. Introduction

Laryngeal squamous cell carcinoma (LSCC) is the second most common type of malignant tumor in the head and neck region, with high recurrence and mortality rates [1, 2]. Because the early clinical symptoms are not obvious, many patients already present metastasis at the time of diagnosis [3, 4]. The current treatment options for LSCC include surgical resection, chemotherapy, radiotherapy, and immunotherapy, etc. [5]. Despite certain advancements in these treatment methods, due to delayed diagnosis, the overall 5-year survival rate of patients remains low, particularly for those with advanced or metastatic disease [4, 6]. Therefore, the search for new biomarkers is crucial for improving the prognosis of LSCC. These biomarkers not only aid in early diagnosis but also predict disease progression and guide treatment choices.

Energy metabolism reprogramming is a key area in cancer research, involving cells adjusting metabolic pathways to meet the energy demands of rapid growth and proliferation, and has long been considered an emerging hallmark of cancer [7]. Studies have shown that the aberrant metabolites or intermediates of cancer metabolism may play a significant role in regulating the proliferation, differentiation, activation, and function of immune cells [8, 9]. The composition and density of immune cells in the tumor microenvironment (TME) profoundly affect the progression of tumors and the success of cancer treatments [10]. A recent study has developed a novel metabolism-related signature to predict the prognosis of LSCC [11]. Another study constructed an immune-related gene signature to predict the risk of recurrence for LSCC patients [12]. These studies indicate that metabolism and immunity both play significant roles in the development of LSCC and may, to some extent, jointly participate in the progression of LSCC. However, there are currently no predictive models that consider the combination of metabolic and immune genes. Therefore, exploring the joint effects of metabolic and immune genes, as well as how they collectively influence the development and treatment response of LSCC, is a direction worth further investigation. This could provide important scientific evidence for the development of new therapeutic strategies and prognostic assessment tools.

In this study, we aimed to establish a prognostic signature for LSCC by combining immune-related genes (IRGs) and metabolism-related genes (MRGs). After confirming its prognostic implication, we further explored the significance of this prognostic model in relation to immunological characteristics, the efficacy of immunotherapy, somatic mutation, and drug sensitivity. In conclusion, this model enriches the theoretical framework for LSCC treatment and contributes to more precise antitumor therapy.

2. Methods

2.1 Data Acquisition and Processing

By accessing The Cancer Genome Atlas (TCGA) database (https://portal.gdc.cancer.gov/), we extracted RNA sequencing and clinical data, as well as mutation data, from 116 LSCC and 12 normal tissue samples. We downloaded the expression matrix and clinical information of GSE25727 [13] from the Gene Expression Omnibus (GEO) database (https://www.ncbi.nlm.nih.gov/geo/). We downloaded 1973 IRGs from the ImmPort Resources database (https://www.immport.org/) (Supplementary Table 1). We also obtained 944 MRGs by searching relevant literature [14] (Supplementary Table 2). Subsequently, using the "limma" package in R software (version 4.4.1), we performed differential expression analysis on the TCGA-LSCC cohort. After identifying the differentially expressed genes (DEGs), we intersected these DEGs with MRGs and IRGs to obtain the DEGs related to both immunity and metabolism. We further analyzed the correlation among these genes. Additionally, we explored the potential molecular mechanisms underlying the disease through Kyoto Encyclopedia of Genes and Genomes (KEGG) and Gene Ontology (GO) enrichment analyses.

2.2 Construction and Validation of the Prognostic Model

First, we used univariate Cox analysis to identify potential genes associated with patient prognosis. Next, we further filtered these candidate genes using the Lasso-Cox regression method to reduce the issue of multicollinearity in the model. Finally, we used multivariate Cox analysis to obtain the optimal risk score model. The risk score was calculated based on the following formula: Risk Score = $\sum$ (gene expression level × corresponding coefficient) [15]. In all cohorts, samples were divided into low-risk and high-risk groups based on the median value of the risk score. To assess the accuracy of the grouping, we performed principal component analysis on the risk genes. Kaplan-Meier analysis was used to compare the overall survival between the two risk subgroups. The "Survival" package was employed to draw receiver operating characteristic (ROC) curves to validate the accuracy of the model's predictions. The predictive model was externally validated using the GEO dataset GSE25727 to test its stability.

2.3 Independent Prognostic Analysis and Nomogram Construction

We combined clinical and pathological information and used univariate and multivariate Cox regression analyses to determine whether the predictive effect of the prognostic signature was independent of clinical variables. Subsequently, we used the "rms" R package to construct a nomogram to predict the 1-, 3-, and 5-year survival rates for patients in the TCGA-

LSCC cohort. Additionally, we performed stratified analyses of clinical features to evaluate the prognostic value of the prognostic model in different subgroups stratified by clinical characteristics.

2.4 Immune Analysis

In the TCGA cohort, we used the “maftools” package to calculate the gene mutation profiles of patients in the high-risk and low-risk groups. To understand the immune cell infiltration in LSCC tumors, we employed several currently recognized immune infiltration scoring methods, including XCELL, TIMER, QUANTISEQ, MCPCOUNT, EPIC, CIBERSORT, and CIBERSORT-ABS. Spearman correlation analysis was used to examine the correlation between immune cells and risk scores. Single-sample gene set enrichment analysis (ssGSEA) was employed to quantify the relative infiltration levels of 28 immune cell subtypes in the TME. The ESTIMATE algorithm was used to assess the immune score and stromal score. We used the Tumor Immune Dysfunction and Exclusion (TIDE) database (http://tide.dfci.harvard.edu/) to calculate the TIDE scores for each TCGA-LSCC sample and compared the differences in TIDE scores between the two groups. Additionally, we compared the levels of immune checkpoint genes between the two risk groups.

2.5 Drug Sensitivity Analysis

Half-maximal inhibitory concentration (IC50) values for frequently used chemotherapeutic agents were calculated using the “pRRophetic” R package [16]. Drug sensitivities were compared between the risk groups, and statistical significance was assessed using the Wilcoxon test.

3. Results

3.1 Identification and Analysis of Immune and Metabolism-related Differentially Expressed Genes in LSCC

A total of 6990 DEGs were identified with FDR <0.05 as the screening criteria (Figure 1A). By intersecting the DEGs from LSCC with IRGs and MRGs, we obtained a total of 12 immune and metabolism-related genes (IMRGs) (Figure 1B). The correlation analysis of these 12 genes is shown in Figure 1C, with salmon color indicating positive correlation and ice blue indicating negative correlation. Functional enrichment analysis revealed that GO terms were primarily enriched in processes such as glycerophospholipid metabolism, epithelial cell migration, cell projection membrane, cell leading edge, phospholipase activity, and lipase activity (Figure 1D). KEGG analysis showed significant enrichment in pathways such as the vascular endothelial growth factor (VEGF) signaling pathway, FcεRI signaling pathway, and inositol phosphate metabolism (Figure 1E). These pathways are all related to immunity and metabolism.

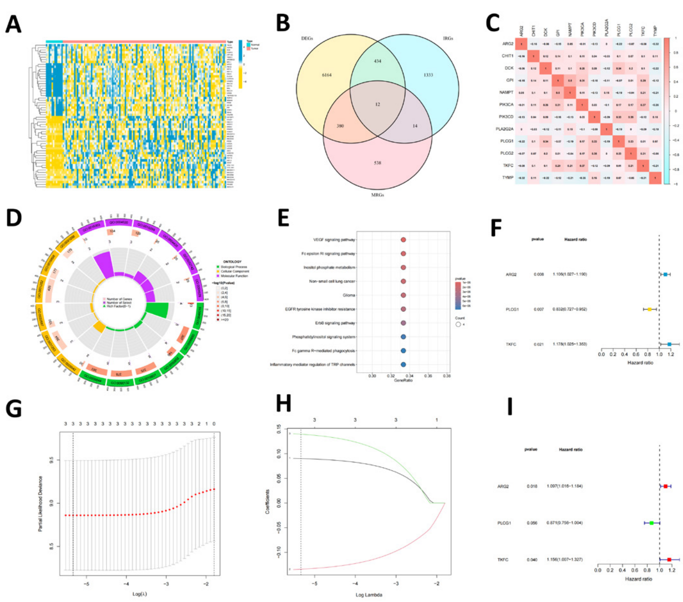

Figure 1. Prognostic Gene Screening and Enrichment Analysis. (A) Heatmap of DEGs in TCGA-LSCC. (B) Venn diagram showing the intersection of DEGs with IRGs and MRGs. (C) Heatmap depicting the correlation of differentially expressed IMRGs. (D) GO enrichment analysis. (E) KEGG pathway enrichment analysis. (F) Univariate Cox regression analysis. (G-H) LASSO regression analysis. (I) Multivariate Cox regression analysis.

3.2 Construction and Validation of the Prognostic Model

Subsequently, we performed univariate Cox analysis on the 12-IMRGs ($p<0.05$, Figure 1F), followed by LASSO regression analysis (Figure 1G, H) and multivariate Cox analysis (Figure 1I). Ultimately, we identified three prognostic immune and metabolism-related genes (ARG2, PLCG1, TKFC), with PLCG1 being lowly expressed in LSCC, while ARG2 and TKFC were highly expressed. Based on these three genes, we constructed a prognostic scoring model to assess risk: Risk Score = (0.0926×expression level of ARG2) + (-0.1382×expression level of PLCG1) + (0.1448×expression level of TKFC). Then, according to the median value of the risk score, LSCC patients were divided into high-risk and low-risk groups. Heatmap analysis showed significant differences in the expression of the three genes between the high-and low-risk groups (Figure 2A). Principal component analysis (PCA) confirmed that samples with different risk scores were separated into two groups (Figure 2B). In the risk score distribution and survival status plot (Figure 2C), more death events were observed in the high-risk group, indicating that an increased risk score reflected an unfavorable prognosis for LSCC patients. Kaplan-Meier curve analysis revealed a significant difference between the two predicted risk groups, with the low-risk group having better overall survival (OS) than the high-risk group ($p<0.001$; Figure 2D). The area under the ROC curve for the risk score was 0.655 (Figure 2E), suggesting good risk prediction performance of the model. Subsequent time-dependent ROC curves showed area under the curve (AUC) values of 0.647, 0.731, and 0.754 for 1-,3-, and 5-year predicted survival rates, respectively (Figure 2F), demonstrating the strong prognostic power of the signature. We also used the dataset GSE25727 as an external validation set to verify our results. Based on the median value of the aforementioned risk score, patients in the validation set were divided into high-risk and low-risk groups (Figure 2G,H). Consistent with the previous results, more recurrence events were observed in the high-risk group in the validation set (Figure 2I), and the disease-free survival rate was significantly higher in the low-risk group than in the high-risk group ($p=0.023$; Figure 2J). The area under the ROC curve was also 0.655 (Figure 2K), with AUC values of 0.583, 0.603, and 0.648 for predicting 1-, 3-, and 5-year recurrence rates, respectively (Figure 2L). These results indicated that the risk score was also applicable to LSCC recurrence patients.

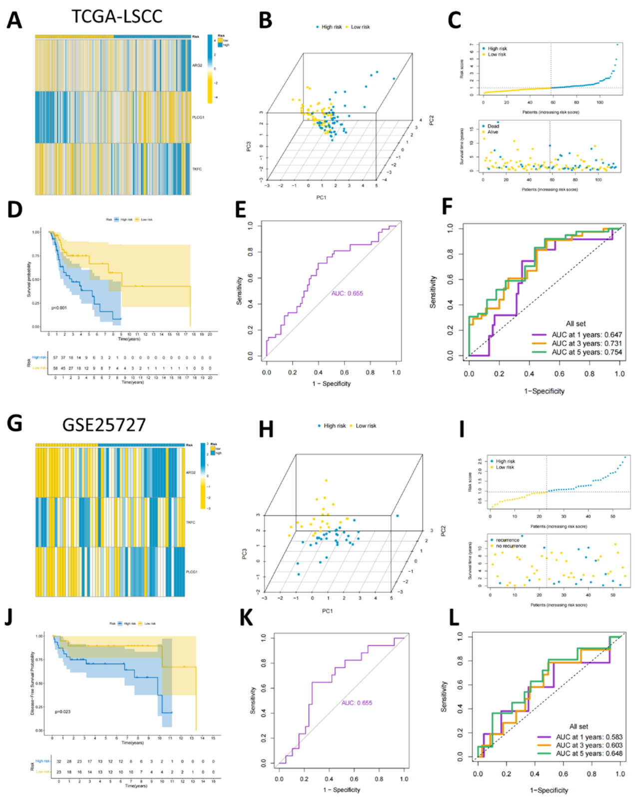

Figure 2. Validation of the prognostic model. (A, G) Heatmaps of expression differences between high-risk and low-risk groups of prognostic genes. (B, H) PCAnalysis. (C, I) Scatter plots showing the distribution of risk scores and survival status. (D, J) Kaplan-Meier survival curves for high-risk and low-risk groups of patients. (E, K) ROC curves of the prognostic model. (F, L) Time-dependent ROC curves of the prognostic model at 1, 3, and 5 years. (TCGA-LSCC cohort: A, B, C, D, E, F; GSE25727 cohort: G, H, I, J, K, L).

3.3 Independent Prognostic Analysis and Nomogram Construction

We evaluated the independent predictive value of the prognostic model through univariate and multivariate Cox analyses. The results showed that the risk score was an independent predictor of poor OS in both analyses. The results of the univariate Cox analysis were as follows: hazard ratio (HR) = 1.507, 95% confidence interval (CI): 1.226 - 1.853 (Figure 3A). The results of the multivariate Cox analysis were as follows: HR = 1.647, 95% CI: 1.188 - 2.283 (Figure 3B). To accurately predict the probability of patient survival, we constructed a nomogram that included the risk score and other clinical and pathological features (including gender, age, and stage) and drew calibration curves (Figure 3C, D) to evaluate survival at 1, 3, and 5 years. The results showed that the OS of LSCC patients decreased over time, and the calibration curves confirmed the accuracy and specificity of the nomogram. Additionally, we further explored the correlation between the risk score and clinical features. The results showed that the risk score was closely related to clinical features (Figure 3E).

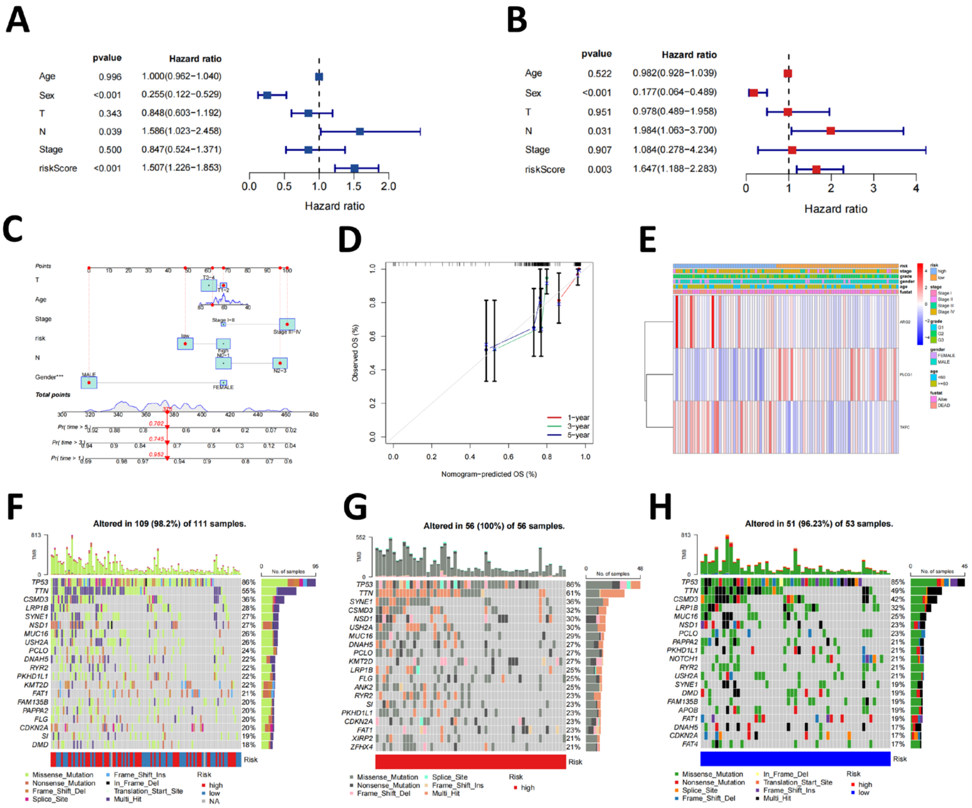

Figure 3. Independent prognostic analysis and nomogram construction, mutation analysis. (A) Univariate Cox analysis of risk scores and clinical features. (B) Multivariate analysis for independent prognostic factors. (C) Prognostic nomogram. (D) Calibration curve of the nomogram. (E) Heatmap of risk scores and clinicopathological features. (F) Waterfall plot of mutation frequency differences between high-risk and low-risk groups. (G) Waterfall plot of mutation frequency in the high-risk group. (H) Waterfall plot of mutation frequency in the low-risk group. (*$p < 0.001$).**

3.4 Immune Analysis

The results of the mutation analysis showed that there were differences in tumor gene mutations between the two risk groups, with a higher mutation rate in the high-risk group (Figure 3F-H). Tumor immune cell infiltration is widely recognized as one of the important immune characteristics of the TME. Through Spearman correlation analysis using multiple algorithms, we sought to find the correlation between risk scores and immune cell abundance in the LSCC TME. Among them, CD8+ T cells were negatively correlated with risk scores in XCELL, TIMER, MCPCOUNT, and CIBERSORT-ABS, and positively correlated in EPIC. M1 and M2 macrophages were negatively correlated with risk scores in XCELL, QUANTISEQ, and CIBERSORT-ABS (Figure 4A). To understand the distribution and correlation of the relative content of 22 types of tumor-infiltrating immune cells in LSCC, we applied the CIBERSORT algorithm to calculate the infiltration of immune cells in the samples. The results showed that naive B cells, plasma cells, naive CD4+ T cells, activated natural killer (NK) cells, resting memory CD4+ T cells, activated memory CD4+ T cells, resting dendritic cells, γδ T cells, M0 and M1 and M2 type macrophages had higher levels of immune infiltration in the low-risk group. In contrast, resting mast cells, activated mast cells, memory B cells, monocytes, CD8+ T cells, follicular helper T cells, regulatory T cells, activated dendritic cells, resting natural killer cells, neutrophils, and eosinophils had higher infiltration levels in the high-risk group. Among them, M1 macrophages, follicular helper T cells, and activated dendritic cells were statistically significant (Figure 4B, C). Differences in immune cell infiltration may lead to changes in immune function. Therefore, we compared the ssGSEA scores of immune functions, and the majority of immune function scores in the low-risk group were significantly higher than those in the high-risk group (Figure 4D, E). At the same time, we further investigated the relationship between the risk model and the TME in the two groups of patients. Compared with patients in the high-risk group, patients in the low-risk group had higher ESTIMATE scores, immune scores, and stromal scores (Figure 4F), indicating that the immune system was more active and robust in patients with lower risk scores. Meanwhile, we used TIDE to score all samples. After comparing the TIDE scores of the high- and low-risk groups, we found that patients in the low-risk group had higher scores, which may mean that they have a stronger ability in immune evasion and may have a poorer response to immunotherapy (Figure 4G, P=0.0027). These results indicate that the IMRGs risk score model can classify different immune subtypes, thereby affecting the response to immunotherapy. In addition, given that immune checkpoints and their ligands are potential therapeutic targets, we examined their relationship with immune checkpoint inhibitors (ICIs). The results showed significant differences in immune checkpoints between the high- and low-risk groups, and the vast majority of immune checkpoint genes (including CTLA4, PDCD1LG2, LAG3, TIGIT, etc.) were upregulated in the low-risk group ($p < 0.05$, Figure 4H). This suggests that the risk score grouping related to immune and metabolism may be used as a potential biomarker for immune checkpoint blockade therapy.

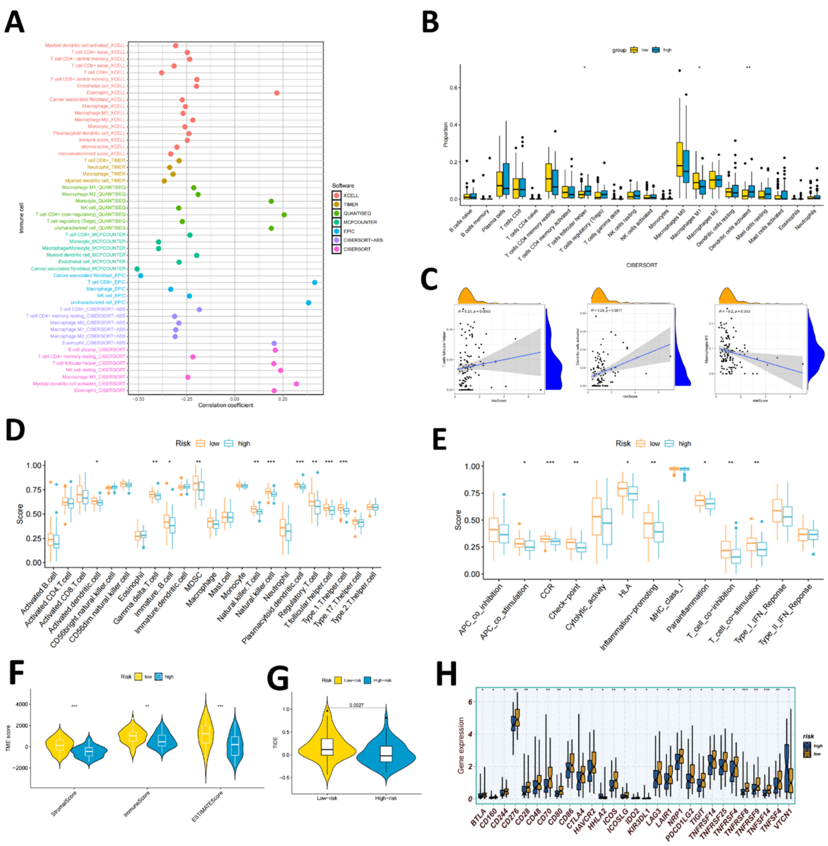

Figure 4. Immune cell infiltration analysis. (A) Multiple algorithms showing the correlation analysis between risk scores and immune cell infiltration. (B) The differences of immune cells infiltration between two risk groups in boxplots. (C) The correlations between immune cells infiltration and risk scores. (D, E) Box plot of the expression levels of 23 immune cell types 13 immune functions between two risk groups by ssGSEA. (F) TME score plot for the two risk groups. (G) Difference plot of TIDE scores between the two risk groups. (H) Expression levels of immune checkpoints between the two risk groups. (*$p < 0.05$; **$p < 0.01$; *$p < 0.001$).

3.5 Drug Sensitivity Analysis

By calculating the IC50 for each LSCC patient in the two groups, we identified 6 drugs with significant differences: GW.441756 (a tropomyosin-related kinase A inhibitor), PF.4708671 (an S6K1 inhibitor), AMG.706 (motesanib), GDC0941 (a PI3K inhibitor), PF.02341066 (crizotinib), and NU.7441 (a DNA-PK inhibitor) ($p < 0.001$, Figure 5A-F). Among them, the high-risk group had lower IC50 values for the tropomyosin-related kinase A inhibitor and the S6K1 inhibitor, suggesting that patients in the high-risk group may benefit from these drugs. In contrast, the IC50 values for motesanib, the PI3K inhibitor, crizotinib, and the DNA-PK inhibitor were higher in the high-risk group, indicating that patients in this group may not benefit from these drugs.

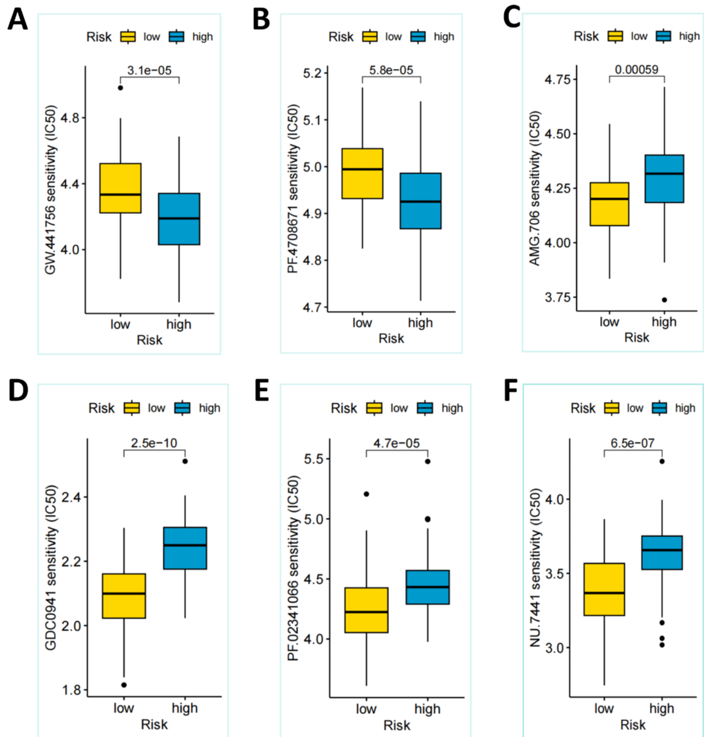

Figure 5. Drug sensitivity analysis. (A) Tropomyosin-related kinase A inhibitor (GW.441756). (B) S6K1 inhibitor (PF.4708671). (C) Motesanib (AMG.706). (D) PI3K inhibitor (GDC0941). (E) Crizotinib (PF.02341066). (F) DNA-PK inhibitor (NU.7441).

4. Discussion

Previous studies have indicated that metabolic reprogramming plays a role in cancer development and that metabolism-related genes can serve as prognostic markers [11, 17]. Immune cells undergo metabolic reprogramming during proliferation, differentiation, and the execution of effector functions, which is crucial for immune responses [7]. During cancer progression, tumor cells and tumor-infiltrating lymphocytes, including CD8+ T cells, regulatory T cells, and natural killer cells, rewire their metabolic programs in response to microenvironmental stressors such as nutrient deprivation and hypoxia. Tumor cells alter their nutrient and metabolic pathways to meet their energetic, biosynthetic, and antioxidant demands. Similarly, metabolic processes in immune cells support the host's immune response to cancer [18].

In this study, we identified 12 DEGs related to both immunity and metabolism through screening. GO enrichment analysis indicated that these DEGs were primarily enriched in processes such as glycerophospholipid metabolism, cell projection membrane, and phospholipase activity. Glycerophospholipids are major components of cell membranes and provide important signaling molecules [19]. Tumor cells exhibit metabolic changes associated with malignancy, including the development of a lipogenic phenotype. Highly proliferative cancer cells require the de novo synthesis of fatty acids to continuously supply glycerophospholipids, especially for membrane biogenesis [20]. Glycerophospholipid metabolism has been shown to regulate various functions, such as adhesion, migration, apoptosis, and signal transduction, thereby affecting tumor progression [21]. This is consistent with our findings. KEGG analysis revealed that the DEGs related to both immunity and metabolism were primarily enriched in the VEGF signaling pathway. Previous studies have confirmed that VEGF plays a crucial role in normal embryonic angiogenesis as well as in the pathological angiogenesis of many diseases, including cancer [22]. VEGF is an important cytokine in the TME, with cancer cells and tumor-associated macrophages being the main sources of VEGF [23, 24]. Activation of the VEGF signaling pathway not only promotes tumor angiogenesis but is also associated with the aggressiveness and metastatic potential of tumors. During tumor progression, VEGF binds to its receptors to activate downstream signaling pathways, thereby promoting the proliferation, migration, and survival of vascular endothelial cells, processes that are crucial for tumor angiogenesis [22, 25]. VEGF can directly affect a variety of immune-related cells, including dendritic cells, T cells, regulatory T cells, and myeloid-derived suppressor cells [26]. In addition, VEGF can influence the expression of immunologically important molecules by endothelial cells, reducing the expression of vascular cell adhesion molecule 1, which is vital for the adhesion and infiltration of anti-cancer T cells into the tumor. VEGF inhibition has been shown to increase the number of tumor-infiltrating lymphocytes in animal models and humans, thereby affecting tumor progression [27-29]. In cancer therapy, blocking the VEGF signaling pathway has become a promising treatment strategy. A recent study demonstrated that the combination of PD-1 antibody, HDAC inhibitor, and VEGF antibody showed potential efficacy in patients with metastatic colorectal cancer. This combination therapy enhanced CD8+T cell infiltration, leading to a more immunologically active TME [30]. In the context of LSCC, VEGF-C, due to its non-invasiveness and rapid accessibility, may be used as an indicator for the diagnosis and monitoring of LSCC [31]. High expression of angiogenic biomarkers is associated with reduced survival and increased recurrence rates; thus, angiogenic biomarkers may help identify high-risk patients, especially in early-stage LSCC [32]. Another study showed that downregulation of miR-206 promotes the proliferation and invasion of laryngeal cancer by regulating VEGF expression [33]. These results all support the reliability of our study.

Subsequently, through stepwise regression analysis, we identified three genes (ARG2, PLCG1, TKFC) to construct our prognostic model, which demonstrated good predictive capability. In our study, we found that the aforementioned three immune and metabolism-related genes were associated with tumor prognosis, consistent with previous research findings. ARG2, also known as arginase 2, is an enzyme that functions in the TME and is abnormally upregulated in various types of cancer. It affects the function of immune cells by regulating arginine metabolism and plays a key role in the regulation of tumor growth and metastasis [34]. High transcriptional levels of ARG2 are associated with low levels of cytotoxic T cells and T cells, which may impact tumor immune surveillance and the effectiveness of immunotherapy [35]. Increased activity of ARG2 in tumors is commonly associated with more advanced disease and poorer clinical outcomes, including head and neck squamous cell carcinoma, breast cancer, liver cancer, and gastric cancer [36-40]. Additionally, experiments in mice have demonstrated that activating pro-inflammatory ARG2-specific CD4 T cells that react to ARG2-derived peptides can inhibit tumor growth [41]. These findings suggest that ARG2 may have similar prognostic value in LSCC, with its expression levels potentially related to the aggressiveness and metastatic potential of the tumor. PLCG1 (phospholipase C γ 1) regulates extracellular signal-regulated kinase, mitogen-activated protein kinase, and nuclear factor of activated T cells signaling pathways, playing a key role in maintaining immune homeostasis [42]. In previously constructed LSCC immune-related prognostic models, low expression levels of PLCG1 may affect prognosis through immune-related pathways [43]. Moreover, PLCG1 expression can serve as a prognostic biomarker for patients with advanced oral squamous cell carcinoma [44] and myelodysplastic syndromes [45], with reduced PLCG1 expression associated with lower survival rates. This is consistent with our findings of low PLCG1 expression. TKFC, a bifunctional enzyme involved in fructose metabolism, can regulate the antiviral immune response by interacting with IFIH1 (MDA5) [46]. Studies have shown that circSOBP inhibits the progression of glioma by binding to the TKFC protein to suppress glycolysis and activate MDA5-mediated immune responses [47]. Additionally, comprehensive computational modeling has revealed a correlation between TKFC and the prognosis of hepatocellular carcinoma [48]. These results further support the reliability of our study.

To sum up, the development and validation of this prognostic model, which integrates immune and metabolic factors, has significantly enhanced our comprehension of the therapeutic landscape for LSCC. It also furnishes robust scientific backing for the implementation of more targeted anti-tumor therapeutic approaches. By employing this multifaceted analytical methodology, we are better equipped to unravel the intricacies of LSCC and to devise treatment plans that are more tailored to individual patients.

Admittedly, there are some limitations in this study. For example, the model we developed was based on and validated against data from public databases. As such, additional clinical data will be essential for further corroborating our findings in the future. Moreover, the validity of our research outcomes needs to be substantiated through both in vivo and in vitro molecular studies.

Declarations

Ethics Approval and Consent to Participate

Not applicable.

Human and Animal Rights

Not applicable.

Consent for Publication

All authors have read and agreed to the published version of the manuscript.

Availability of Data and Materials

All relevant data supporting the findings presented in this study are available within the article and its Supplementary Information files, or from the corresponding author upon reasonable request.

Authors' Contributions

Made substantial contributions to conception and design of the study and performed data analysis and manuscript writing: Zhang Feng and Zhenlian Xie; contributed to the data analysis, figure generation, and literature search: Shiwei Gong; revised the manuscript: Zhang Feng. All authors have read and agreed to the published version of the manuscript.

Conflict of Interest

The authors declare no conflict of interest, financial or otherwise.

References

[1] Wang JQ, Lan L, Ma B, et al. KRT17 accelerates cell proliferative and invasive potential of laryngeal squamous cell carcinoma through regulating AKT/mTOR and Wnt/β-catenin pathways. Evid Based Complement Alternat Med. 2022;2022:6176043.

[2] Bray F, Ferlay J, Soerjomataram I, et al. Global cancer statistics 2018: GLOBOCAN estimates of incidence and mortality worldwide for 36 cancers in 185 countries. CA Cancer J Clin. 2018;68(6):394-424.

[3] Cavaliere M, Bisogno A, Scarpa A, et al. Biomarkers of laryngeal squamous cell carcinoma: a review. Ann Diagn Pathol. 2021;54:151787.

[4] Jiang X, Jiang W. The construction and validation of ECM-related prognosis model in laryngeal squamous cell carcinoma. Heliyon. 2023;9(9):e19907.

[5] Dai F, Xie Z, Yang Q, et al. MicroRNA-375 inhibits laryngeal squamous cell carcinoma progression via targeting CST1. Braz J Otorhinolaryngol. 2022;88(Suppl 4):S108-16.

[6] Zhao R, Yang Z, Zhao B, et al. A novel tyrosine tRNA-derived fragment, tRFTyr, induces oncogenesis and lactate accumulation in LSCC by interacting with LDHA. Cell Mol Biol Lett. 2023;28(1):49.

[7] Xia L, Oyang L, Lin J, et al. The cancer metabolic reprogramming and immune response. Mol Cancer. 2021;20:1-21.

[8] Cronin SJF, Seehus C, Weidinger A, et al. The metabolite BH4 controls T cell proliferation in autoimmunity and cancer. Nature. 2018;563(7732):564-8.

[9] Oliveira LM, Teixeira FME, Sato MN. Impact of retinoic acid on immune cells and inflammatory diseases. Mediators Inflamm. 2018;2018:3067126.

[10] Sturm G, Finotello F, Petitprez F, et al. Comprehensive evaluation of transcriptome-based cell-type quantification methods for immuno-oncology. Bioinformatics. 2019;35(14):i436-45.

[11] Shen Y, Huang Q, Zhang Y, et al. A novel signature derived from metabolism-related genes GPT and SMS to predict prognosis of laryngeal squamous cell carcinoma. Cancer Cell Int. 2022;22(1):226.

[12] Hong X, Li Y, Lv Q, et al. Identification of an immune-related genes signature to predict risk of recurrence for patients with laryngeal squamous cell carcinoma. Int J Immunopathol Pharmacol. 2023;37:03946320231172075.

[13] Fountzilas E, Markou K, Vlachtsis K, et al. Identification and validation of gene expression models that predict clinical outcome in patients with early-stage laryngeal cancer. Ann Oncol. 2012;23(8):2146-53.

[14] Huang H, Zhou S, Zhao X, et al. Construction of a metabolism-related gene prognostic model to predict survival of pancreatic cancer patients. Heliyon. 2023;9(1):e12378.

[15] Wu P, Sun W, Zhang H. An immune-related prognostic signature for thyroid carcinoma to predict survival and response to immune checkpoint inhibitors. Cancer Immunol Immunother. 2022;71(3):747-59.

[16] Geeleher P, Cox NJ, Huang RS. Clinical drug response can be predicted using baseline gene expression levels and in vitro drug sensitivity in cell lines. Genome Biol. 2014;15:R47.

[17] Li JD, Chen Y, Jing SW, et al. Triosephosphate isomerase 1 may be a risk predictor in laryngeal squamous cell carcinoma: a multi-centered study integrating bulk RNA, single-cell RNA, and protein immunohistochemistry. Eur J Med Res. 2023;28(1):591.

[18] Chuang YM, Tzeng SF, Ho PC, et al. Immunosurveillance encounters cancer metabolism. EMBO Rep. 2024;25(2):471-88.

[19] Mukhopadhyay TK, Trauner D. Concise synthesis of glycerophospholipids. J Org Chem. 2022;88(15):11253-7.

[20] Dolce V, Cappello AR, Lappano R, et al. Glycerophospholipid synthesis as a novel drug target against cancer. Curr Mol Pharmacol. 2011;4(3):167-75.

[21] Perrotti F, Rosa C, Cicalini I, et al. Advances in lipidomics for cancer biomarkers discovery. Int J Mol Sci. 2016;17(12):1992.

[22] Holash J, Davis S, Papadopoulos N, et al. VEGF-Trap: a VEGF blocker with potent antitumor effects. Proc Natl Acad Sci U S A. 2002;99(17):11393-8.

[23] Valković T, Dobrila F, Melato M, et al. Correlation between vascular endothelial growth factor, angiogenesis, and tumor-associated macrophages in invasive ductal breast carcinoma. Virchows Arch. 2002;440:583-8.

[24] Shieh YS, Hung YJ, Hsieh CB, et al. Tumor-associated macrophage correlated with angiogenesis and progression of mucoepidermoid carcinoma of salivary glands. Ann Surg Oncol. 2009;16:751-60.

[25] Deryugina EI, Quigley JP. Tumor angiogenesis: MMP-mediated induction of intravasation-and metastasis-sustaining neovasculature. Matrix Biol. 2015;44:94-112.

[26] Khan KA, Kerbel RS. Improving immunotherapy outcomes with anti-angiogenic treatments and vice versa. Nat Rev Clin Oncol. 2018;15(5):310-24.

[27] Chung AS, Wu X, Zhuang G, et al. An interleukin-17-mediated paracrine network promotes tumor resistance to anti-angiogenic therapy. Nat Med. 2013;19(9):1114-23.

[28] Shrimali RK, Yu Z, Theoret MR, et al. Antiangiogenic agents can increase lymphocyte infiltration into tumor and enhance the effectiveness of adoptive immunotherapy of cancer. Cancer Res. 2010;70(15):6171-80.

[29] Wallin JJ, Bendell JC, Funke R, et al. Atezolizumab in combination with bevacizumab enhances antigen-specific T-cell migration in metastatic renal cell carcinoma. Nat Commun. 2016;7:12624.

[30] Wang F, Jin Y, Wang M, et al. Combined anti-PD-1, HDAC inhibitor and anti-VEGF for MSS/pMMR colorectal cancer: a randomized phase 2 trial. Nat Med. 2024;30(4):1035-43.

[31] Huang Q, Ji M, Li F, et al. Diagnostic and prognostic value of plasma cell-free DNA combined with VEGF-C in laryngeal squamous cell carcinoma. Mol Cell Probes. 2023;67:101895.

[32] Schlüter A, Weller P, Kanaan O, et al. CD31 and VEGF are prognostic biomarkers in early-stage, but not in late-stage, laryngeal squamous cell carcinoma. BMC Cancer. 2018;18(1):272.

[33] Zhang T, Liu M, Wang C, et al. Down-regulation of MiR-206 promotes proliferation and invasion of laryngeal cancer by regulating VEGF expression. Anticancer Res. 2011;31(11):3859-63.

[34] Niu F, Yu Y, Li Z, et al. Arginase: An emerging and promising therapeutic target for cancer treatment. Biomed Pharmacother. 2022;149:112840.

[35] Giatromanolaki A, Harris AL, Koukourakis MI. The prognostic and therapeutic implications of distinct patterns of argininosuccinate synthase 1 (ASS1) and arginase-2 (ARG2) expression by cancer cells and tumor stroma in non-small-cell lung cancer. Cancer Metab. 2021;9(1):28.

[36] Grzywa TM, Sosnowska A, Matryba P, et al. Myeloid cell-derived arginase in cancer immune response. Front Immunol. 2020;11:938.

[37] Bron L, Jandus C, Andrejevic-Blant S, et al. Prognostic value of arginase-II expression and regulatory T-cell infiltration in head and neck squamous cell carcinoma. Int J Cancer. 2013;132(3):E85-93.

[38] Giannoudis A, Varešlija D, Sharma V, et al. Characterisation of the immune microenvironment of primary breast cancer and brain metastasis reveals depleted T-cell response associated to ARG2 expression. ESMO Open. 2022;7(6):100636.

[39] Tang Y, Xu L, Ren Y, et al. Identification and validation of a prognostic model based on three MVI-related genes in hepatocellular carcinoma. Int J Biol Sci. 2022;18(1):261-75.

[40] Zhang J, Jin Y, Xu S, et al. AGR2 is associated with gastric cancer progression and poor survival. Oncol Lett. 2016;11(3):2075-83.

[41] Weis-Banke SE, Lisle TL, Perez-Penco M, et al. Arginase-2-specific cytotoxic T cells specifically recognize functional regulatory T cells. J Immunother Cancer. 2022;10(10):e005326.

[42] Tao P, Han X, Wang Q, et al. A gain-of-function variation in PLCG1 causes a new immune dysregulation disease. J Allergy Clin Immunol.

2023;152(5):1292-302.

[43] Sun M, Chen S, Fu M. Model establishment of prognostic-related immune genes in laryngeal squamous cell carcinoma. Medicine (Baltimore). 2021;100(2):e24263.

[44] Zhu D, Tan Y, Yang X, et al. Phospholipase C gamma 1 is a potential prognostic biomarker for patients with locally advanced and resectable oral squamous cell carcinoma. Int J Oral Maxillofac Surg. 2014;43(12):1418-26.

[45] Shiseki M, Ishii M, Miyazaki M, et al. Reduced PLCG1 expression is associated with inferior survival for myelodysplastic syndromes. Cancer Med. 2020;9(2):460-8.

[46] Tremblay-Laganière C, Michaud C, Abourjaili-Bilodeau R, et al. Homozygous variant in TKFC abolishing triokinase activities is associated with isolated immunodeficiency. J Med Genet. 2024.

[47] Mu M, Niu W, Chu F, et al. CircSOBP suppresses the progression of glioma by disrupting glycolysis and promoting the MDA5-mediated immune response. iScience. 2023;26(10):107897.

[48] Walakira A, Skubic C, Nadižar N, et al. Integrative computational modeling to unravel novel potential biomarkers in hepatocellular carcinoma. Comput Biol Med. 2023;159:106957.

Appendix (Supplementary Information)

Supplementary Table 1: 1973 immune-related genes.

Immune-related genes
AZGP1
B2M
CALR
CANX
CD1A
CD1B
CD1C
CD1D
CD1E
CD4
CD8A
CD8B
CD74
CREB1
CTSB
CTSE
CTSL
CTSS
FCER1G
FCGRT
PDIA3
HFE
HLA-A
HLA-B
HLA-C
HLA-DMA
HLA-DMB
HLA-DOA
HLA-DOB
HLA-DPA1
HLA-DPB1
HLA-DQA1
HLA-DQA2
HLA-DQB1
HLA-DRA
HLA-DRB1
HLA-DRB3
HLA-DRB4
HLA-DRB5
HLA-E
HLA-F
HLA-G
HLA-H
MR1
HSPA1A
HSPA1B

Supplementary Table 2: 944 metabolism-related genes.

Metabolism-related genes
AKR1C4
PRODH
NME6
GK
CKMT1A
PAICS
CES1
TYMP
GLS2
POLR2D
SAT1
UAP1
DGKG
UPB1
AKR1B10
TH
POLD4
PLA2G5
LIPF
ACAT1
UGT2B7
PIP4K2C
NT5C
ARG1
DNMT3L
DHRS4L2
RDH10
PNLIPRP1
CES2
ADH1B
CMPK2
UGT2B17
ADCY9
PGM2L1
CNDP1
GSTZ1
CPOX
ENPP7
BST1
ACOX3
GSTA3
ENTPD6
HMGCS2
GNPAT
ALOX12B
MCEE